Research Article

T. Arumuga Maria Devi* and V. I. Mebin Jose

Three Stream Network Model for Lung Cancer Classification in the CT Images

https://doi.org/10.1515/comp-2020-0145
Received Apr 15, 2020; accepted Jul 23, 2020

Abstract: Lung cancer is considered to be one of the deadly diseases that threaten the survival of human beings. It is a challenging task to identify lung cancer in its early stage from the medical images because of the ambiguity in the lung regions. This paper proposes a new architecture to detect lung cancer obtained from the CT images. The proposed architecture has a three-stream network to extract the manual and automated features from the images. Among these three streams, automated feature extraction as well as the classification is done using residual deep neural network and custom deep neural network. Whereas the manual features are the handcrafted features obtained using high and low-frequency sub-bands in the frequency domain that are classified using a Support Vector Machine Classifier. This makes the architecture robust enough to capture all the important features required to classify lung cancer from the input image. Hence, there is no chance of missing feature information. Finally, all the obtained prediction scores are combined by weighted based fusion. The experimental results show 98.2% classification accuracy which is relatively higher in comparison to other existing methods.

Keywords: Convolutional Neural Network (CNN), Lung Cancer,Computerized Tomography (CT), Support Vector Machine (SVM), Deep Neural Network (DNN)

1 Introduction

Lung cancer is considered as one of the major threats to human health on a worldwide scale [1]. As declared by the World Health Organization (WHO), 7.6 million of the total population dies each year because of this cancer [2]. Because of the lacking early diagnosis and proper medical treatment to the patients, it is estimated that lung cancer may threaten the livelihood of more than 17 million populations worldwide by 2030 [3]. Lung cancer can be grouped into Non-Small Cell Lung Cancer (NSCLC) [4] and Small Cell Lung Cancer (SCLC). NSCLC is further grouped into squamous cell cancer, large cell cancer, and lung adenocarcinoma. The treatment of varied groups of this lung cancer differs based on the early screening of the carcinoma and its impact. Right, and early pathological diagnosis can actualize a viable treatment design and drag outpatient survival [5]. Medical imaging advances in high-resolution image acquisition modalities coupled with emerging image processing standards can contribute to the medical society as well as save the life of the patient. High-resolution Computer Tomography (CT) and X-ray chest radiography are the principal anatomic imaging modalities that are normally utilized for diagnosing different lung ailments. Among the emerging medical image processing standards, AI-based deep learning [6] has evolved to be the best in the diagnosis of carcinoma with minimal human intervention. In line with the visual inspection of the cancerous lesion images by the medical experts, deep learning can naturally distinguish complex patterns [7]. Therefore, early detection of lung cancer after proper image acquisition involves the development of a non-invasive computer-aided diagnosis [8] system that uses recent deep learning algorithms to solve complex problems. Deep learning methods are free of handcrafted carcinoma feature extraction methods. Deep learning-based Convolution Neural Networks require a lot of input medical images to extract low level to high-level features during training the networks. But due to the lack of a vast number of input images, transfer learning is used to increase the classification accuracy of lung carcinoma [9]. Hence, the computer-aided diagnosis (CAD) systems using deep learning methods improve the accuracy of diagnosis and cut costs in a short period of time [10]. Also, a single deep neural network will not make much impact on early detection, so a hybrid detection framework using a three stream deep neural network model is proposed in this paper. The major contributions of this paper are outlined as follows;

(i) A base residual deep neural network is used along with a custom Deep Neural Network (DNN). Transfer

***Corresponding Author: T. Arumuga Maria Devi:** Manonmanium Sundaranar University, India; Email: deviececite@gmail.com
V. I. Mebin Jose: Manonmanium Sundaranar University, India; Email: josemebin@gmail.com

learning is performed on the residual network and fine tuned on the lung cancer dataset to perform automatic feature extraction. The custom DNN extracts the features from the scratch.
(ii) Manual feature extraction with Support Vector Machine (SVM) [11, 12] classifier is adopted to improve the CAD system performance.
(iii) In this three stream model, the results obtained from all the three streams are combined to predict the tumors as cancerous or non-cancerous.
(iv) The performance of individual architectures, as well as the proposed three stream architecture, is evaluated on a standard database for lung cancer diagnosis.

This paper is organized as follows. Section 2 states the review of the existing literature and Section 3 describes the proposed method. Section 4 provides the results and discussion and Section 5 concludes the work. In the past various image processing and pattern recognition algorithms emerged to predict the occurrence of lung cancer in its early stages. But among these lung cancer classification approaches, pattern recognition based methods showed improved performance over the classical image classification algorithms. Pattern recognition based methods are further classified into machine learning and deep learning approaches. These two approaches are extensively reviewed in this paper.

2 Literature reviews

2.1 Machine learning approaches

The machine learning approaches are mainly based on different handcrafted features and supervised classifiers such as Artificial Neural Network (ANN), Support Vector Machine, and Nearest Neighborhood. These classifiers should be trained with specific features to get proper classification performance. The existing machine learning techniques that are focused on lung cancer classification are discussed. In ANN, the input features play a significant role. Also, it is complex and requires a lot of computations. ANN based ensemble is proposed by Zhou *et al.* [13] to obtain high accuracy in the classification of carcinoma. Zhu *et al.* [14] selected 25 features based on the textures in Solitary Pulmonary Nodules (SPN) obtained from the CT images that are classified using the SVM classifier. Similarly, Shao *et al.* [15] proposed an automated framework to detect the SPN effectively using the SVM classifier. Orozco *et al.* [16] used features obtained from the wavelet transform to feed it to the SVM for further classification of lung cancer. Features extracted from the gabor filters are given to the K-nearest neighborhood (KNN), a classifier that is optimized using genetic algorithms [17]. The genetic algorithm depends on mutation which is unsupervised. Akram, Javed, and Hussain [18] used thresholding to segment the portion of the lung nodules which is a trial and error method. Later, features are extracted from these regions and fed to the ANN to reach an accuracy of 88.37%. Carvalho Filho *et al.* [19] utilized taxonomic diversity and distinct criteria to classify lung cancer using SVM classifiers. It shows an accuracy of 98.11%. Sangamithraa and Govindaraju [20] used Gray Level Co-occurrence Matrix (GLCM) to extract the features and it is fed to a Back Propagation Network to get 90.7% accuracy in classification.

2.2 Deep Learning approaches

Deep learning approaches work without any handcrafted features; it automatically extracts the features from the images. This approach is categorized as Traditional CNN, Hybrid CNN, and Transfer learning CNN. The Traditional CNN implies a single deep neural network structure which is a combination of different convolutional layers. Hybrid CNN is the combination of two or more deep neural networks. Transfer Learning CNN is a pretained network that can be fine-tuned by addition/deletion of layers and setting various hyperparameters as per the requirements.

2.2.1 CNN

In this section, traditional CNNs and their performance measures are reviewed extensively. Jin *et al.* [21] proposed a Convolutional Neural Network (CNN) that classifies lung cancer using three convolutional layers for feature extraction. Here, there is lack of learning the necessary feature information, therefore it provides an accuracy of 84.6%. Stacked Denoising Autoencoder, CNN, and Deep Belief Networks are used to classify lung cancer by Sun *et al.* [22]. Deep Belief Network performed well compared to the other two methods such as SDA and CNN. But over fitting reduced the accuracy to 81.19%. Golan, Jacob, and Denzinger [23] used CNN for classification, but it gave only 78.9% accuracy. Even though existing methods that help in the early identification of lung cancer shows appropriate performance, there is still a need to develop a robust lung cancer classification system that can yield far better performance. Anthimopoulos *et al.* [24] used CNN to classify different lung tissues with 85.61% accuracy. A multi-scale and multistream DNN was proposed by Ciompi *et al.* for the efficient classification of six different types of lung nodules with good accuracy values [25]. Song *et al.* [6] have used deep learning-based techniques to classify lung cancer. Most of the recent deep learning techniques for the efficient classification of lung cancer are reviewed by Riquelme and Akhloufi [26]. Asuntha and Srinivasan extracted the features for lung cancer classification using Local Binary Pattern (LBP), Scale Invariant Feature Transform, Histogram of oriented Gradients (HoG), wavelet transform-based features, and Zernike Moment [27]. From the extracted set of features, Fuzzy Particle Swarm Optimization is used for feature selection. Finally, these features are given as inputs to the deep learning-based classifier for the classification of lung cancer.

2.2.2 Hybrid CNN

This section exclusively reviews that the Hybrid CNNs and their performance measures. Polat and Danaei Mehr. [28] proposed a 3D deep CNN that uses softmax and a hybrid 3D deep CNN that uses SVM for lung cancer classification. In comparison, 3D hybrid CNN with SVM achieves the highest accuracy of 91.81%. Zhao *et al.* [29] proposed a hybrid CNN which is the combination of LeNet and Alexnet. Both network architectures are combined for better feature learning and classification. The overall accuracy of this method is 82.23% for optimal parameter settings. Qin *et al.* [30] proposed Fine-grained features for classification of lung cancer. Multidimensional attention is used to reduce the feature noise while extracting fine-grained features from the PET and CT scans for classification. Effective feature extraction is performed using this technique.

2.2.3 Transfer Learning CNN

This section provides that the Transfer learning CNNs and their performance measures. Wang *et al.* [31] used the transfer learning approach to fine-tune the residual network that provides the result with an accuracy of 0.9575. Here, the short connection network improves classification performance. Fang [32] used Google network as the base network to get good accuracy and fast convergence. Then the network is fine-tuned and applied to examine the malignancy of lung cancer and obtained an accuracy of 80%. Nóbrega *et al.* [33] fine tuned most of the CNN models like VGG16, VGG19, MobileNet, Xception, InceptionV3, ResNet50, Inception-ResNet-V2, DenseNet169, DenseNet201, NASNetMobile, and NASNetLarge. The Xception network with MLP provides better accuracy of 89.91%, but still, this accuracy value is low. In this paper, a hybrid three stream deep neural network is proposed to overcome the limitations such as the lack of learning important features and misclassification rate. Among the three network architecture, even if one fails to predict correctly, the other two can make the entire network to predict the lung cancer effectively because of fusion. So there is no chance of missing features in this method.

3 Proposed method

In this paper, a three stream deep neural network model is proposed to classify lung cancer obtained from the lung CT images [15]. This model consists of three different architecture which is the combination of one machine learning and two deep learning architectures. The block diagram is shown in Figure 1. The machine learning architecture provides the handcrafted features and the deep learning system provides the automatic features that are needed for the classification of lung CT medical images. Since the essential features from both the automatic as well as the artificial features are extracted, there is no chance of missing important or robust information. This leads to an improvement in the classification accuracy.

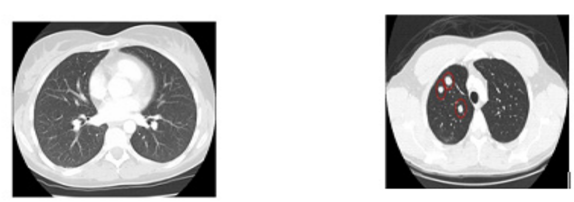

(a) Noncancerous image (b) Cancerous image

Figure 1: Sample lung CT images.

The deep learning architecture used for automatic feature extraction uses a CNN that uses transfer learning. Here ResNet is used that is fine-tuned for lung cancer classification. Additionally, a custom CNN that is learned from scratch is used to boost the performance of the network by making significant changes in the overall accuracy. Also the machine learning architecture uses spatial and frequency-based features to be fed to SVM for classification. Finally, all the predicted scores from three network are combined by weighted based fusion.

3.1 Preparation of Dataset and Preprocessing

For lung cancer classification, the LIDC/IDRI database is used. It consists of 1018 sample images. For training, 80% of the dataset is used, and the remaining 20% is used for testing. The training images are augmented using rotation, flipping, resizing, and translation. All the images are resized into 256×256. A sample image of both normal and malignant lung nodules is shown in Figure 2. Image preprocessing is performing after converting the image to the frequency domain. Un-decimated Discrete Wavelet Transform (UDWT) is used for frequency conversion.

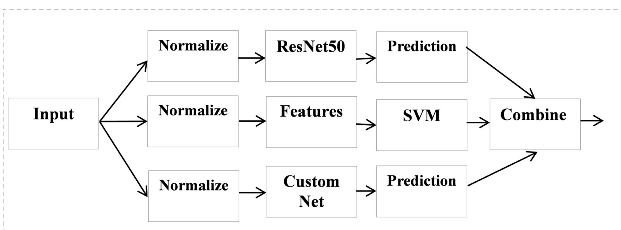

Figure 2: Proposed Tri stream deep network-based model.

For preprocessing the training images, two methods are used here. The first one is the Contrast Limited Adaptive Histogram Equalization (CLAHE) [34, 35] and the other is the Z-score normalization. Preprocessing enhances the image, and then Inverse Un-decimated Discrete Wavelet Transform (IUDWT) is applied. Equalization cum normalization gives better contrast-enhanced images for better training [36, 37] The Z-score normalization is defined by;

$$Z(i) = \frac{(x(i) - mean(x))}{std(x)} \quad (1)$$

where i ranges from 1 to n, x is feature value and std refers to standard deviation.

3.2 Basic CNN Architecture

CNN architecture is generally composed of the convolutional layer, which is the building block, Rectified Linear Unit (ReLU) activation function, and pooling layers. Convolutional layers are used to extract low-level features to high-level features. A depth of many convolutional layers is used to extract these features. This gives an adequate information of the entire image. The ReLU layers help to allow significant information to the next stage. It provides non-linearity to the network. The pooling layer is used to minimize the dimension to reduce computational complexity.

3.3 Residual Architecture for classification

A fine tuned Residual neural network is used as the first stream in this tri-stream deep network model. ResNet is a deep neural network that has a significant connection, *i.e.*, skip or short connection over the network layers, unlike conventional deep neural networks. ResNet is able to train the images with more than 50 layers successfully. It is given in Table 1. Instead of increasing network depth by simply stacking layers together, ResNet introduces an “identity shortcut connection” that skips one or more layers. It is shown in the following Figure 3. This identity connection is very much helpful to avoid the vanishing gradients problems in the network by using the previous layer activations until the present layer learns its weights.

Table 1: Feature sets.

Sl.no	Features
1	Energy
2	Entropy
3	Skewness
4	Kurtosis
5	Average

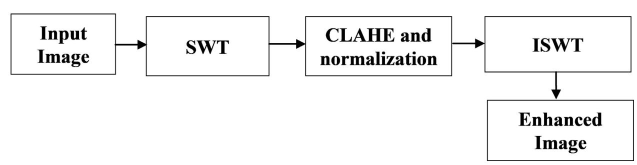

Figure 3: Method of Preprocessing.

During training, the weights adapt to mute the upstream layer and amplify the previously-skipped layer. In the simplest case, only the weights for the adjacent layer’s connection are adapted, with no exact weights for the upstream layer. Skipping effectively simplifies the network, using fewer layers in the initial training stages.This speeds learning by reducing the impact of vanishing gradients, as there are fewer layers to propagate through. The network then gradually restores the skipped layers as it learns the feature space. Towards the end of the training, when all layers are expanded, it stays closer to the manifold and thus learns faster. The pre-trained ResNet50 is fine-tuned in the last layers as well as in the fully connected layer to perform the lung cancer classification. It automatically extracts low level to high-level features related to the lung nodules. The skip connection is shown in Figure 4. The

Figure 5 represents the different number of layers in the Residual networks.

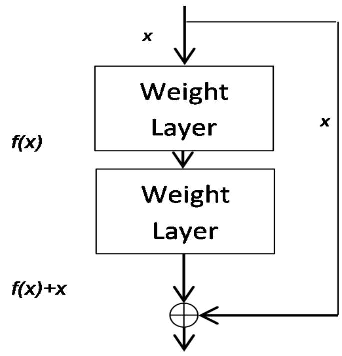

Figure 4: Identity connections in the ResNet.

layer name	output size	18-layer	34-layer	50-layer	101-layer	152-layer
conv1	112×112	7×7, 64, stride 2				
conv2_x	56×56	3×3 max pool, stride 2				
		$\begin{bmatrix} 3\times3, 64 \\ 3\times3, 64 \end{bmatrix}\times2$	$\begin{bmatrix} 3\times3, 64 \\ 3\times3, 64 \end{bmatrix}\times3$	$\begin{bmatrix} 1\times1, 64 \\ 3\times3, 64 \\ 1\times1, 256 \end{bmatrix}\times3$	$\begin{bmatrix} 1\times1, 64 \\ 3\times3, 64 \\ 1\times1, 256 \end{bmatrix}\times3$	$\begin{bmatrix} 1\times1, 64 \\ 3\times3, 64 \\ 1\times1, 256 \end{bmatrix}\times3$
conv3_x	28×28	$\begin{bmatrix} 3\times3, 128 \\ 3\times3, 128 \end{bmatrix}\times2$	$\begin{bmatrix} 3\times3, 128 \\ 3\times3, 128 \end{bmatrix}\times4$	$\begin{bmatrix} 1\times1, 128 \\ 3\times3, 128 \\ 1\times1, 512 \end{bmatrix}\times4$	$\begin{bmatrix} 1\times1, 128 \\ 3\times3, 128 \\ 1\times1, 512 \end{bmatrix}\times4$	$\begin{bmatrix} 1\times1, 128 \\ 3\times3, 128 \\ 1\times1, 512 \end{bmatrix}\times8$
conv4_x	14×14	$\begin{bmatrix} 3\times3, 256 \\ 3\times3, 256 \end{bmatrix}\times2$	$\begin{bmatrix} 3\times3, 256 \\ 3\times3, 256 \end{bmatrix}\times6$	$\begin{bmatrix} 1\times1, 256 \\ 3\times3, 256 \\ 1\times1, 1024 \end{bmatrix}\times6$	$\begin{bmatrix} 1\times1, 256 \\ 3\times3, 256 \\ 1\times1, 1024 \end{bmatrix}\times23$	$\begin{bmatrix} 1\times1, 256 \\ 3\times3, 256 \\ 1\times1, 1024 \end{bmatrix}\times36$
conv5_x	7×7	$\begin{bmatrix} 3\times3, 512 \\ 3\times3, 512 \end{bmatrix}\times2$	$\begin{bmatrix} 3\times3, 512 \\ 3\times3, 512 \end{bmatrix}\times3$	$\begin{bmatrix} 1\times1, 512 \\ 3\times3, 512 \\ 1\times1, 2048 \end{bmatrix}\times3$	$\begin{bmatrix} 1\times1, 512 \\ 3\times3, 512 \\ 1\times1, 2048 \end{bmatrix}\times3$	$\begin{bmatrix} 1\times1, 512 \\ 3\times3, 512 \\ 1\times1, 2048 \end{bmatrix}\times3$
	1×1	average pool, 1000-d fc, softmax				
FLOPs		1.8×10^9	3.6×10^9	3.8×10^9	7.6×10^9	11.3×10^9

Figure 5: Transfer learning model ResNet-18, 34, 50, 101, 152.

3.4 Machine learning architecture

This machine learning architecture [38, 39] is the second stream of the proposed model. The artificial features are calculated from both the spatial [12] and frequency domain. The frequency-domain conversion is carried out by Un-decimated Discrete Wavelet Transform (UDWT). The features that are extracted in both low frequency and high-frequency sub-bands are listed in Table 1. The Energy (EN), Entropy (ENP), and Average (AVG) feature sets are expressed in equation (2), (3), (4).

$$EN = \frac{1}{p^2.q^2}\sum_{x=1}^{p}\sum_{y=1}^{q}|Fv(x,y)|^2 \tag{2}$$

$$ENP = \sum_{i=1}^{p} P(Fv(x,y)).log(Fv(x,y)) \tag{3}$$

$$AVG = \frac{1}{p.q}\sum_{x=1}^{p}\sum_{y=1}^{q} Fv(x,y) \tag{4}$$

Where, EN = Energy, ENP = Entropy, AVG = Average, $Fv(x, y)$ = Frequency values of wavelets, p = image width, q = image height

3.4.1 Local Binary Patterns

Local binary patterns (LBP) are used to identify the texture information from the images. This texture feature is very important to train the classifier. Here the LBP operator is used to extract the texture information in both frequency and spatial domain. Three different radiuses R (3, 5, and 7) are used for texture extraction using LBP operators in both the low and high-frequency wavelet coefficients. In total 55 features (10+30+15=55) are extracted to train the SVM classifier. SVM is a supervised classifier that uses a radial basis function as the linear kernel.

3.5 Custom DNN for lung cancer classification

The custom DNN architecture forms the third stream of the tri stream deep neural network. It is used to extract the essential low level, mid-level, and high-level features automatically using the convolutional layers. The layers used in the custom DNN are given in Table 2. The kernel size of all layers is 3×3, and the number of filters in each convolutional layer is 256, 256, 512, 512, and 512 respectively. The first three convolutional layers have the ReLU activation function, and the last two convolutional layers have the leaky ReLU activation function. Figure 6 shows the block diagram of the custom DNN architecture. The en-

Table 2: Layers in Custom DNN.

Layer	Feature map	Size	Kernel size
Input image		256×256×3	
Convolution	128	3×3×3	3×3
Channel norm		10	
Max pooling		3	
Convolution	256	3×3×256	3×3
Convolution	256	3×3×256	3×3
Max pooling		3	
Convolution	512	3×3×512	3×3
Convolution	512	3×3×512	3×3
Max pooling		3	
Fully connected		1000	
Fully connected		1000	
Fully connected		2	

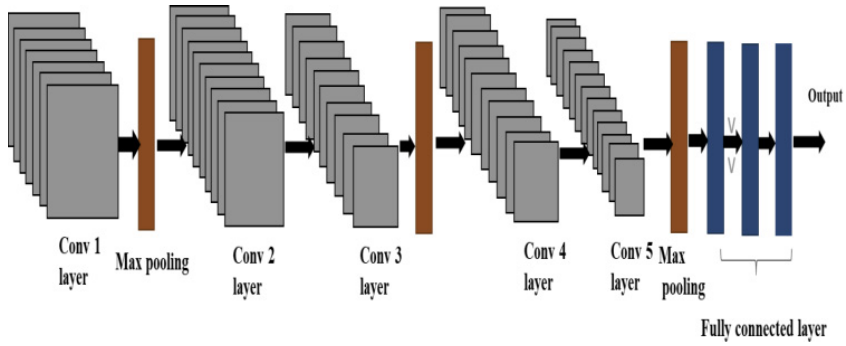

Figure 6: Architecture of proposed custom deep neural network.

tire training image is normalized by Z-score normalize, and classification is done by softmax classifier. The first and second fully connected layer has 1000 connections. It acts as the neural network classifier. The third fully connected layer represents the number of classes, here it is two. It is found that the augmented training data provide better results after performing training on both the augmented and raw training data.

3.5.1 Training Algorithm

1. Input: Training data samples (Tds) with no. of image class labels (nI), Validation sets (Vds), Learning Rate (Lr), Optimizer.
2. Output-Feature map, performance parameters such as accuracy, sensitivity, specificity.
3. Train the network with Adam optimizer to reduce the cross-entropy loss.
4. Calculate Loss on training data set (Tds) and validation data sets (Vds) by backpropagation based on the correct class labels.
5. Initialize the learning Rate (Lr).
6. For X = 1 to no of images (nI).
   (a) Take the feature map for the last convolutional layer.
   (b) Find softmax of the ouput layer.
7. Return Loss, Accuracy, probabilistic feature map.

3.5.2 Fusion

A weighted average fuses all the prediction score of three network streams in the proposed model. Since the SVM classifier has the least chance of accurate detection, the other two deep neural networks have an almost similar capability. Therefore, the average of all the prediction scores decides the final classification results.

4 Results and discussion

4.1 Performance measures

In this paper, the proposed architecture is evaluated using metrics such as Accuracy (Acc), Specificity (Spec), and Sensitivity (Sen). It is expressed in equation (5), (6), (7). Here, TN, FP, TN, and FN denote True positive, False Positive, True Negative, and False Negative, respectively.

$$Accuracy(Acc) = \frac{TP}{TP + TN + FP + FN} \tag{5}$$

$$Specificity(Spec) = \frac{TN}{TN + FP} \tag{6}$$

$$Sensitivity(Sen) = \frac{TP}{TP + FN} \tag{7}$$

4.2 Training

The augmented dataset is given as input to the three-stream architecture for feature extraction and prediction. Then the obtained prediction scores are combined using weighted fusion to classify the cancerous or non-cancerous samples. The experiment is carried out using MATLAB 2019 in an NVIDIA GEFORCE GPU. Adam optimization is used to minimize the error and train the network efficiently. In this paper, the used batch size is 32, learning a rate of 0.0001, 100 epochs, and momentum 0.9.

4.3 Testing

The trained model is tested on the test dataset to prove its efficiency using the performance metrics. The experiments are carried out by random splitting of training and testing data by 80% and 20% in both the augmented and non-augmented datasets. The comparison of the performance metrics values before performing augmentation is tabulated in Table 3.

Table 3: Performance metric comparison with out augmentation.

Method	Acc	Spec	Sens
Resnet-50	86	85	89
Customnet	89	82	91
SVM	85	81	87
Proposed	96.3	94	94.5

From Table 3, it is understood that SVM attains the lowest performance metrics such as the least accuracy sensitivity specificity values. ResNet performs slightly better than SVM but comparatively lower than the custom net. But the combination of the three-stream network perform well compared to separate architecture with an accuracy of 96.3% and a sensitivity value of 94.0% and specificity value of 94.5%. Similarly, Table 4 shows the performance of the individual streams and the combined model after performing image augmentation on the input image. It is seen that the performance achieved is similar to Table 3 but the accuracy, sensitivity, and specificity values are slightly increased. It is because of the huge dataset of images used for training by data augmentation. This lifts the performance values in comparison to those results obtained without performing augmentation.

Table 4: Performance metric comparison with augmentation.

Method	Acc	Spec	Sens
Resnet-50	87	86	90
Customnet	90	84.9	91.1
SVM	86.5	83.4	89.2
Proposed	98.2	99	96.5

The performance metrics are also tabulated for different transfer learning architectures such as Alexnet, ResNet, and VGG in Table 5 and Table 6. Table 5 shows the performance without augmented data, and Table 6 shows the performance measures with augmented data. The proposed framework performs better in terms of all metric values compared to other transfer learning networks. The Residual network performance is high in comparison to VGG and Alexnet because of the presence of short connections. Here, even if some of the features are lost in the presentation layer, the previous layer features are added with the next layer to eliminate the vanishing gradients. These connections aids in learning all the essential and important features from every stage. Figure 7 represents the progress of the training process. The validation loss is decreasing for each iteration which reveals that the error minimizes. Also from the first half of the Figure 7, it can be seen that the accuracy increases when the loss keeps on reducing.

Table 5: Performance metric comparison among various network without augmented data.

Method	Acc	Spec	Sens
Alexnet	87.5	87	88.5
Resnet-152	93	92	92.5
VGG-16	89.5	90.3	90
Proposed	96.3	94	94.5

Table 6: Performance metric comparison among various network with augmented data.

Method	Acc	Spec	Sens
Alexnet	91.5	92	92.8
Resnet-152	96	95.6	94.5
VGG-16	92.8	92.4	93.5
Proposed	98.2	99	96.5

Figure 8 shows the ROC curve for the proposed full/tri stream deep network model. The obtained AUC for this model is 97.93% which is higher than the other one stream and two-stream network.

Figure 9 shows the ROC curve for the proposed network model together with ResNet and VGG models. The AUC for the proposed is higher than ResNet and VGG deep network. The performance metrics are tabulated for different combination streams without and with augmentation in Tables 7 and 8. The accuracy of the proposed framework with augmentation attains a peak value of 98.2%. From the experimental results, it is concluded that the addition of augmented training data improves the performance of the classification system. Also, the combination of the proposed three-stream architecture leads to improvement in the classification accuracy in comparison to all other networks and existing systems.

The confusion matrix in Figure 10 is used to visualize the performance of the system in most of the machine learning classification problems. This confusion matrix depends

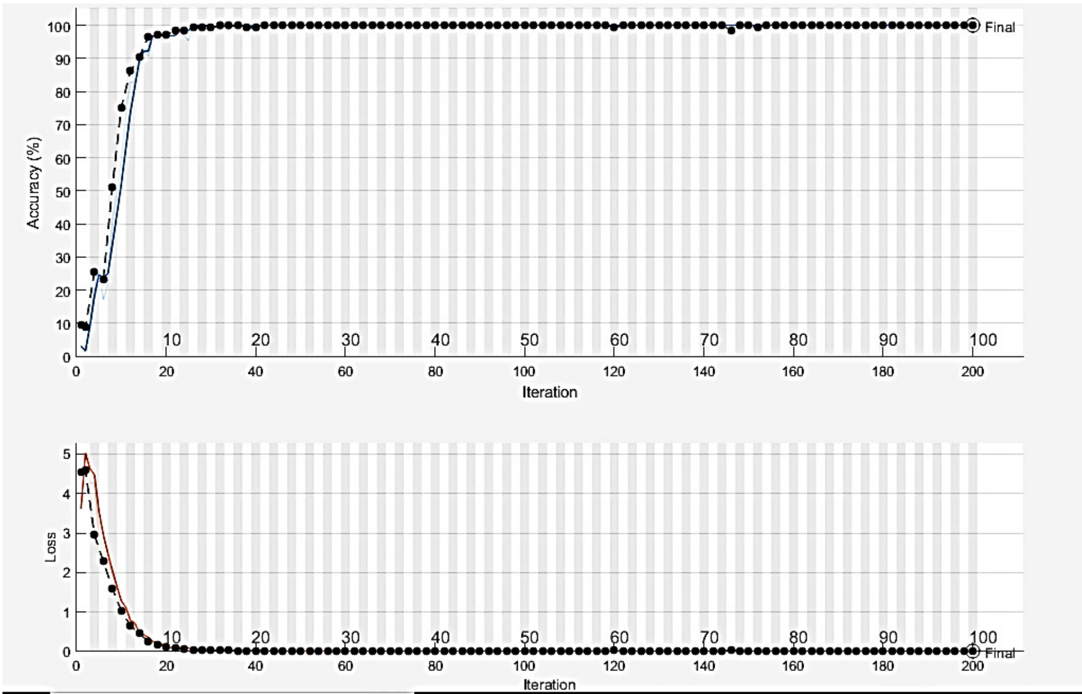

Figure 7: Training Progress – Training Accuracy and Loss.

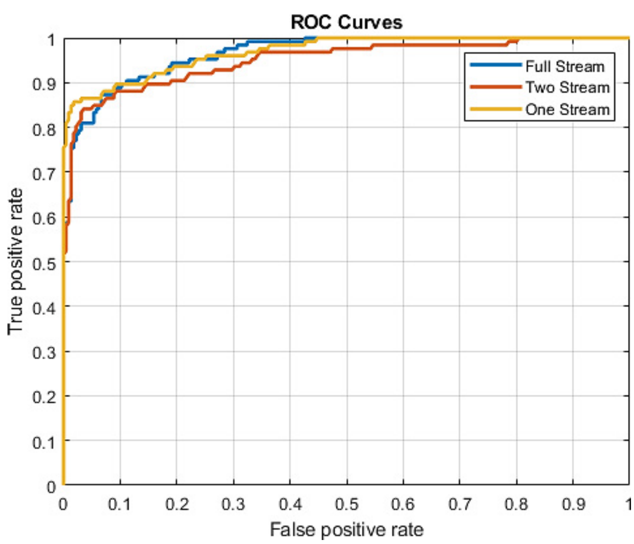

Figure 8: ROC Comparison of different streams.

Table 7: Performance metric comparison among different stream combination without augmented Data.

Method	Acc	Spec	Sens
Stream1+Stream2	87	87.5	90.5
Stream1+Stream3	85	84	88.5
Stream2+Stream3	90.8	88.7	92.3
Proposed	97	95.5	94.8

Table 8: Performance metric comparison among different stream combination with augmented Data.

Method	Acc	Spec	Sens
Stream1+Stream2	91	92	93.5
Stream1+Stream3	90	90.5	91
Stream2+Stream3	91	89	93
Proposed	98.2	99	96.5

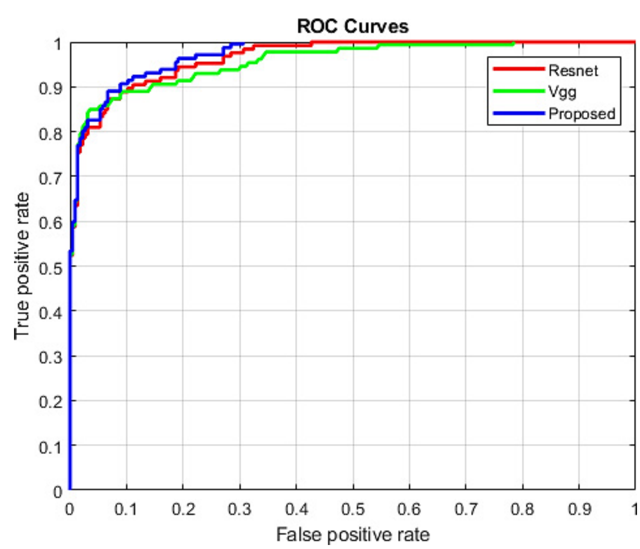

Figure 9: ROC Comparison of three different networks

on the true positive, true negative, false positive, and false-negative vales. Since the two-class problem is formulated here, the confusion matrix will have only two class prediction values. It predicts whether it is healthy or cancerous. It is understood from Figure 10 that among the 1244 normal test samples, 1201 normal samples are identified correctly as normal and the remaining 43 normal samples are identified to be cancerous. Also, from among the 1200 cancerous samples, only one sample is identified wrongly. Therefore, the total accuracy of the system is 98.2%. This system performs well for cancerous samples in comparison to that of healthy samples.

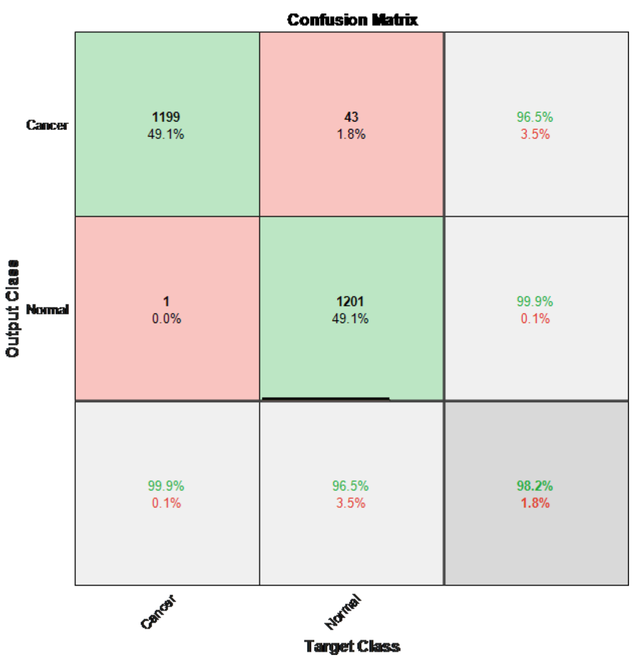

Figure 10: Confusion Matrix of the proposed three stream model.

The performance metrics of the existing systems and the proposed model are tabulated in Table 9. Antonio *et al.* [19] used the taxonomic diversity index and distinction index with the phylogenetic trees to classify lung cancer using SVM. It has the highest specificity and an accuracy of 97.6%. Wenqing *et al.* [22] could achieve 81.19% using Deep Belief Networks. RuoXi Qin [30] proposed a multidimensional attention system that reduces the feature noise while extracting fine-grained features from the PET and CT scans for classification. The Convolutional Neural Network applied for the CT images provides promising results with 92% accuracy. But it is lower than the proposed system because of the use of single structured CNN. This creates a chance of the addition of unwanted features and the elimination of essential features which leads to decreasing the accuracy. Shudong Wang [31] used a system that uses a transfer learning-based residual network and obtained an accuracy of 95.75%. It is 3% lower than the proposed system because the short connections in the residual network sometime over-learns the important features, and it leads to overfitting. Therefore, in conclusion, the proposed three-stream deep network model performs better in terms of accuracy, specificity, sensitivity in comparison to the existing system.

Table 9: Performance metric comparison with existing methods.

Method	Acc	Spec	Sens
Antonio *et al.* [19]	97.6	95.24	97.1
Wenqin *et al.* [22]	81.19	-	-
RuoXi Qin *et al.* [30]	92.0	-	-
Shudong *et al.* [31]	95.75	95.34	96.92
Proposed	98.2	99	96.5

5 Conclusion

The proposed three stream deep network model helps to deeply analyze and produce better feature maps to identify the variation between the normal and abnormal nodules in the lung CT medical images. This leads to an improvement in the classification accuracy because of the combination of the handcrafted and automated features. This also produces a lesser chance of missing valuable information. Hence, this proposed model is potentially very suitable for lung cancer detection in its early stages. Also, this method achieves 98.2% classification accuracy, which is higher compared to the existing methods. In the future, feature-based input can be used instead of raw data which could help the network to learn better. In turn, this could yield reasonable improvements in the performance of the network model.

References

[1] Hoffman PC., Mauer AM., Vokes EE., Lung cancer, Lancet, 2000, 355(9202), 479-485

[2] Nie L., Wang M., Zhang L., Yan S., Zhang B., Chua TS., Disease Inference from Health-Related Questions via Sparse Deep Learning,IEEE Transactions on Knowledge and Data Engineering, 2015, 27(8), 2107–19

[3] Dhaware BU., Pise AC., Lung cancer detection using bayasein classifier and FCM segmentation, International Conference on

Automatic Control and Dynamic Optimization Techniques, (9 Sept – 10 Sept 2016, Pune, India), IEEE, 2016, 170-174
[4] Zhang C., Hao X., Prognostic significance of CD276 in non-small cell lung cancer, Open Medicine, 2019, 14, 805-12
[5] Miller YE., Pathology of Lung Cancer, Clinics in Chest Medicine, 2002, 23(1), 65-81
[6] Song Q., Zhao L., Luo X., Dou X., Using deep learning for classification of lung nodules on computed tomography images, Journal of healthcare engineering, 2017,7,8314740
[7] Litjens G., Kooi T., Bejnordi BE., Setio AA., Ciompi F., Ghafoorian M., Van Der Laak JA., Van Ginneken B., Sánchez CI., A survey on deep learning in medical image analysis, Medical image analysis, 2017, 42, 60–88
[8] Jose MVI., Devi TA., A non invasive computer aided diagnosis system for early detection of lung carcinoma in CT medical images, Int J Latest Trends Eng Technol, 2016, 8(4-1),125-130
[9] Nishio M., Sugiyama O., Yakami M., Ueno S., Kubo T., Kuroda T., Togashi K., Computer-aided diagnosis of lung nodule classification between benign nodule, primary lung cancer, and metastatic lung cancer at different image size using deep convolutional neural network with transfer learning, PLoS ONE, 2018, 13(7)
[10] Cheng JZ., Ni D., Chou YH., Qin J., Tiu CM., Chang YC., Huang CS., Shen D., Chen CM., Computer-aided diagnosis with deep learning architecture: applications to breast lesions in US images and pulmonary nodules in CT scans, 2016, 6(1), 1-13
[11] Devi TA., Jose VM., Parasuraman PK., A novel approach for automatic detection of non-small cell lung carcinoma in CT images, International Conference on Control Instrumentation Communication and Computational Technologies, (16 Dec -17 Dec 2016, Kumaracoil, India), IEEE, 2016, 788-792
[12] Devi TA., Rekha MN., Hyperspectral image classification using spatial and spectral features, International Journal of Scientific and Engineering Research,2013, 4(7),1843
[13] Zhou ZH., Jiang Y., Yang YB., Chen SF., Lung cancer cell identification based on artificial neural network ensembles, Artificial Intelligence in Medicine, 2002, 24(1), 25–36
[14] Zhu Y., Tan Y., Hua Y., Wang M., Zhang G., Zhang J., Feature selection and performance evaluation of support vector machine (SVM)-based classifier for differentiating benign and malignant pulmonary nodules by computed tomography, Journal of digital imaging, 2010, 23(1), 51-65
[15] Shao H., Cao L., Liu Y., A detection approach for solitary pulmonary nodules based on CT images, Proceedings of 2012 2nd International Conference on Computer Science and Network Technology, (29 Dec - 31 Dec 2012, Changchun, China), IEEE, 2012, 1253-1257
[16] Orozco HM., Villegas OO., Sánchez VG., Domínguez HD., Alfaro MD., Automated system for lung nodules classification based on wavelet feature descriptor and support vector machine, Biomedical engineering online, 2015, 14(1)
[17] Bhuvaneswari P., Therese AB., Detection of cancer in lung with k-nn classification using genetic algorithm, Procedia Materials Science, (17 Oct -18 Oct 2014, Mumbai, India), Elsevier, 2015, 433-40.
[18] Akram S., Javed MY., Hussain A., Automated thresholding of lung CT scan for Artificial Neural Network based classification of nodules, (28 June-1 July 2015, Las Vegas, NV, USA), IEEE, 2015, 335-340.
[19] de Carvalho Filho AO., Silva AC., de Paiva AC., Nunes RA., Gattass M., Lung-nodule classification based on computed tomography using taxonomic diversity indexes and an SVM, Journal of Signal Processing Systems, 2017, 87(2), 179-96
[20] Sangamithraa PB., Govindaraju S., Lung tumour detection and classification using EK-Mean clustering, International Conference on Wireless Communications, Signal Processing and Networking, (23 March-25 March 2016, Chennai, India), IEEE, 2016, 23, 2201-2206
[21] Jin XY., Zhang YC., Jin QL., Pulmonary nodule detection based on CT images using convolution neural network, 9th International symposium on computational intelligence and design, (10 Dec-11 Dec 2016, Hangzhou, China), IEEE, 2016, 202-204
[22] Sun W., Zheng B., Qian W., Computer aided lung cancer diagnosis with deep learning algorithms, Proc. SPIE 9785, Medical Imaging 2016: Computer-Aided Diagnosis, 97850Z
[23] Golan R, Jacob C, Denzinger J. Lung nodule detection in CT images using deep convolutional neural networks, 2016 International Joint Conference on Neural Networks (IJCNN), (24 July-29 July 2016, Vancouver, BC, Canada), IEEE, 2016,243–50
[24] Anthimopoulos M., Christodoulidis S., Ebner L., Christe A., Mougiakakou S., Lung pattern classification for interstitial lung diseases using a deep convolutional neural network, IEEE transactions on medical imaging, 2016, 35(5), 1207-16
[25] Ciompi F., Chung K, Van Riel SJ., Setio AA., Gerke PK., Jacobs C., Scholten ET., Schaefer-Prokop C., Wille MM, Marchiano A., Pastorino U., Towards automatic pulmonary nodule management in lung cancer screening with deep learning, Scientific reports, 2017, 7
[26] Riquelme D., Akhloufi MA., Deep learning for lung cancer nodules detection and classification in CT scans, AI, 2020, 1(1), 28-67
[27] Asuntha A., Srinivasan A., Deep learning for lung Cancer detection and classification, Multimedia Tools and Applications, 2020, 1-32
[28] Polat H., Danaei Mehr H., Classification of pulmonary CT images by using hybrid 3D-deep convolutional neural network architecture, Applied Sciences, 2019, 9(5)
[29] Zhao X., Liu L, Qi S., Teng Y., Li J., Qian W., Agile convolutional neural network for pulmonary nodule classification using CT images, International journal of computer assisted radiology and surgery, 2018, 13(4), 585-95
[30] Qin R., Wang Z., Jiang L., Qiao K., Hai J., Chen J., Xu J., Shi D., Yan B., Fine-Grained Lung Cancer Classification from PET and CT Images Based on Multidimensional Attention Mechanism, Complexity, 2020
[31] Wang S., Dong L., Wang X., Wang X., Classification of pathological types of lung cancer from CT images by deep residual neural networks with transfer learning strategy, Open Medicine, 2020,15(1),190-7
[32] Fang T., A novel computer-aided lung cancer detection method based on transfer learning from googlenet and median intensity projections, IEEE International Conference on Computer and Communication Engineering Technology, (18 Aug - 20 Aug 2018, Beijing, China), IEEE, 2018, 286-290
[33] da Nóbrega RV., Peixoto SA., da Silva SP., Rebouças Filho PP., Lung nodule classification via deep transfer learning in CT lung images, IEEE 31st International Symposium on Computer-Based Medical Systems, (18 June - 21 June 2018, Karlstad, Sweden), IEEE, 2018, 244-249
[34] Devi TA., Arumugaraj G., A Novel Technique of Resolution Enhancement in Hyper Spectral Images on proposed CHLAE Technique, Journal of Chemical and Pharmaceutical Sciences, 2016,

9(1),594-597

[35] Devi TA., Arumugaraj G., A modified MSRCR technique for hyper spectral images on various levels of resolution enhancement, International Journal of Advanced Research in Electrical, Electronics and Instrumentation Engineering, 2015, 4(7)

[36] T. Arumuga Maria Devi., S. Benisha,M., Mathan Raja., P. Kuma., E. Senthil Kumar., Meyer Controlled Watershed Segmentation Schistosomiasis in Hyperspectral Data Analysis, International Conference on Control Instrumentation Communication and Computational Technologies, (18th and 19th December 2015, Noorul Islam University, Thuckalay, India), ICCICCT-2015, 829-834

[37] Dr.T. Arumuga Maria Devi., M.Mathan Raja., Simultaneous Visualization and Segmentation of Hyperspectral Data Using Fuzzy K Means Clustering, International Journal for Research in Applied Science and Engineering Technology (IJRASET), 2017, https://europub.co.uk/articles/22035

[38] Dr.T. Arumuga Maria Devi., Diagnosis of Lung Cancer on Big Data Analytics, International Virtual Conference on "Emerging Frontiers in Control and Communication Technologies " Organized by Department of ECE and EEE, (26th August, Mohamed Sathak AJ College of Engineering, India), ICECCT 2020

[39] Hepzibai R., Arumuga Maria Devi T., Darwin P., SenthilKumar E., Detection of Normal and Abnormalities from Diabetics Patient's Foot on Hyperspectral Image Processing. In: Saini H., Sayal R., Buyya R., Aliseri G. (eds) Innovations in Computer Science and Engineering, Lecture Notes in Networks and Systems, Springer, Singapore, 2020, 103